Spatial distribution, source identification, and health risk assessment of fluoride in the drinking groundwater in the Sulin coal district, northern Anhui Province, China

Chunming Hao, Min Liu, Wei Zhang, Peiyong He, Dongjian Lin and Herong Gui

ABSTRACT

Previously, systematic studies of distribution, sources, and health risks of high F^- groundwater used as a drinking-water source in the Sulin coal district, northern Anhui Province of China have not been carried out. In this study, 30 groundwater samples were collected in May 2019, and the data were analyzed using geographic information system, factor analysis, positive matrix factorization, and risk-based corrective action models. The results indicated that the F^- concentration of the groundwater samples ranged from 0.16 to 2.06 mg/L, with a mean value of 1.10 mg/L. The F^- concentrations of 53.33% of the groundwater samples exceeded China's maximum permissible limit for drinking water (1.00 mg/L). Quantificational source apportionment revealed that the weathering of F-bearing minerals is the main source (66.20%). Cation exchange (16.30%), agricultural activities (13.20%), and natural geological processes (4.30%) were the other sources of F^-. The percentages of infants, children, teens, male adults, and female adults that face health risks due to excess F^- intake were approximately 20.00%, 70.00%, 6.67%, 20.00%, and 10.00%, respectively. This research provided useful insights into the proper management of groundwater extraction to mitigate health problems associated with excessive F^- intake.

Key words | fluoride, groundwater, health risk, PMF model, source identification, spatial distribution

Chunming Hao
Min Liu
Wei Zhang
Dongjian Lin
North China Institute of Science and Technology,
Sanhe Hebei 065201,
China

Chunming Hao
State Key Laboratory of Groundwater Protection and Utilization by Coal Mining,
Beijing 100011,
China

Chunming Hao
Herong Gui (corresponding author)
National Engineering Research Center of Coal Mine Water Hazard Controlling,
Suzhou University,
Anhui 234000,
China
E-mail: *guiherong@163.com*

Peiyong He
China Institute of Geo-Environment Monitoring,
Beijing 100081,
China

HIGHLIGHTS

- Quantificational source apportionment of F^- in groundwater was carried out.
- Health risk assessment of F^- exposure was evaluated for individuals in different groups.
- Spatial distribution was analyzed between low and high F^- groundwaters in the Sulin coal district.

INTRODUCTION

Fluorine is the 13th most abundant element in the Earth's crust and the lightest member of the halogen group (Rafique *et al.* 2015; Olaka *et al.* 2016). The daily intake of a trace amount of F^- has positive health benefits, as F participates in the mineralization of bones and teeth. The World Health Organization (WHO) suggests that drinking water with a F^- content of 0.80–1.00 mg/L can improve the dental health of children under the age of 10 (Keshavarzi *et al.* 2010; Mahvi *et al.* 2016; Tiwari *et al.* 2016; Goodarzi *et al.* 2017). However, excessive F^- intake poses health risks (Brindha *et al.* 2016; Dehbandi *et al.* 2018; Yousefi *et al.* 2018). For example, drinking water with a F^- content above 1.50 mg/L over a long period

doi: 10.2166/ws.2021.048

can cause dental fluorosis, and if the F^- content exceeds 4.00 mg/L, it may lead to the development of skeletal fluorosis (Abu & Alsokhny 2004; Keshavarzi *et al.* 2010; Aghapour *et al.* 2018). According to WHO guidelines for drinking-water quality, the maximum permissible limit of F^- in drinking water is 1.50 mg/L (WHO 1984; Keshavarzi *et al.* 2010; Rafique *et al.* 2015; Kumar *et al.* 2018; Rashid *et al.* 2018). In China, approximately 20% of the drinking water is supplied from groundwater (WHO 1984; Zhang *et al.* 2016). However, compared with surface water, the F^- content in groundwater is higher, which can cause health risks (Rafique *et al.* 2015; Aghapour *et al.* 2018). To avoid the potential health risks of excess F^- intake, the Chinese government has set the maximum permissible limit of F^- for drinking water at 1.00 mg/L (Guo *et al.* 2012; He *et al.* 2013a, 2013b).

Several studies have demonstrated that F^- in groundwater mainly originates from weathering of F-bearing minerals (such as fluorite, apatite, micas, and amphibole) (Keshavarzi *et al.* 2010; He *et al.* 2013a; Brindha *et al.* 2016; Dehbandi *et al.* 2018) and anthropogenic activities (such as phosphate fertilizers and pesticides, aluminum smelting, glass and brick industries, coal combustion, and semiconductor industries) (Enalou *et al.* 2018; Thapa *et al.* 2018). Generally, an alkaline environment with low Ca^{2+} content, high Na^+ content, and $NaHCO_3$-type water will increase the F^- content in the groundwater (Rafique *et al.* 2015; Olaka *et al.* 2016; Dehbandi *et al.* 2018; Enalou *et al.* 2018; Kumar *et al.* 2018). In addition, evaporation and ion exchange are two important processes that contribute to an elevated F^- content in groundwater (He *et al.* 2013b; Mondal *et al.* 2014; Olaka *et al.* 2016; Rashid *et al.* 2018).

The distribution, sources, and health risks of high- F^- groundwater in the Hetao Plain (Guo *et al.* 2012; He *et al.* 2013; Tiwari *et al.* 2016), Zhangye Basin (He *et al.* 2013a), Yuncheng Basin (Li *et al.* 2015, 2018), Datong Basin (Pi *et al.* 2015), Yanchi endorheic region (Wu *et al.* 2018), Taiyuan Basin (Li *et al.* 2007), and Wanbei Region (Yang *et al.* 2017) of China, which is one of 25 countries severely affected by F^- contamination, have been widely studied. Studies have shown that the F^- content in almost 73.20% of shallow groundwater samples and 82.70% of deep groundwater samples exceed China's national drinking-water limit (1.0 mg/L) in the northern Anhui Province, China, with maximum F^- contents in shallow and deep groundwaters of 2.85 mg/L and 3.10 mg/L, respectively (Wu *et al.* 2010; Wu & Qian 2011; Yang *et al.* 2017). Due to a lack of effective treatment and protection in the Sulin coal district of the Wanbei Region, over 3.0 million people suffer from dental fluorosis and 100,000 people have developed skeletal fluorosis (Gao *et al.* 2013). The quantitative source apportionment of high F^- groundwater is a challenge. However, factor analysis (FA) combined with a positive matrix factorization (PMF) model provide a solution for quantitative source apportionment of pollutants in soil (Guan *et al.* 2018), water (Rodenburg *et al.* 2011), and sediment (Chen *et al.* 2013).

This study aimed to investigate the distribution of F^- concentrations, perform a quantitative source apportionment, and assess health risks associated with the consumption of groundwater in the Sulin coal district, northern Anhui Province, China, using geographic information systems, PMF, and risk-based corrective action (RBCA) models. The results of this study will contribute to the development of policies for the proper management of groundwater extraction to prevent health risks associated with excess F^- intake.

MATERIALS AND METHODS

Study area

Sulin coal district, with an area of 1,000 km^2, is located in Wanbei, China, and is characterized by a subhumid monsoon climate. The study area extends from 116°15′E to 117°12′E longitude, with a latitude between 33°20′ N and 33°42′N. The annual precipitation is 750–900 mm and the mean annual evaporation is 900–1,050 mm at a mean annual temperature of approximately 14–15 °C. The area lies at an elevation of 20–40 m above sea-level and is dominated by flat terrain. The Tuo River and Hui River are the two main perennial rivers.

The land surface is covered by quaternary sediments with a thickness of 100.50 m to 771.70 m. The multilayer aquifer system in the area consists of both shallow and deep groundwater aquifers. The deep groundwater aquifers consist of sedimentary complexes and alluvial deposits with a mean thickness of 40 m, which are composed of quartz, muscovite, biotite, chlorite, and other minerals. Drinking and irrigation water for rural residents mainly

comes from deep groundwater aquifers. Wheat and corn are the main crops in the study area.

Sample collection and analysis

In total, 30 groundwater samples were collected in the rainy season (May 2019), as shown in Figure 1. During this time, groundwater is at the abundant level period and F^- concentration is active (Table 1). A water level indicator (OTT PLS) was used to measure the groundwater level in open wells. Prior to collection, the groundwater at every sampling site was partially drained to access fresh groundwater. High-density polypropylene bottles used for sampling were first rinsed two or three times with distilled water and then rinsed with groundwater another two or three times. Additionally, all water samples were filtered through filter membranes with a pore size of 0.45 μm before filling the sampling bottles. The samples were usually taken at approximately 0.30 m below the groundwater. For every sampling site, three bottles (500 mL each) were collected. The pH and total dissolved solids (TDS) values were measured in the field using a portable pH meter (OHAUS ST20) and a portable TDS meter (OHAUS ST20T-B), respectively.

The concentrations of anions (Cl^-, SO_4^{2-}, NO_3^-, and F^-) and cations (Ca^{2+}, Mg^{2+}, Na^+, and K^+) were determined by ion chromatography (Dionex Integrion IC, Thermo Fisher, USA) with a detection limit of 0.01 mg/L. The concentrations of carbonate and bicarbonate anions were measured using acid–base titrations in an analytical laboratory with a detection limit of 0.01 mg/L. The analytical

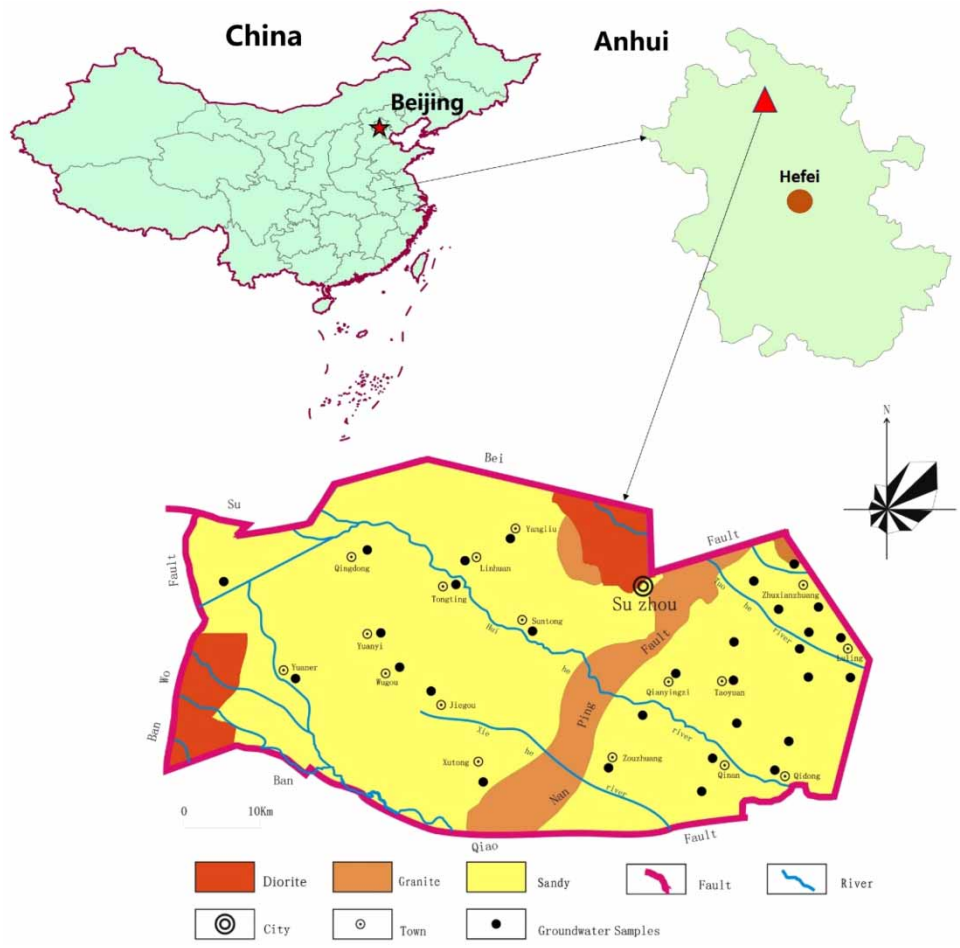

Figure 1 | Locations of the study area.

Table 1 | Hydrological record and fluoride content of groundwater from monitoring area in 2019

Parameters	Rainy season	Dry season
Average rainfall (mm)	630	210
Water elevation (m)	−10.84 to 9.26	−13.68 to 11.41
F^- concentration (mg/L)	0.16–2.06	0.19–1.19 (Gao *et al.* 2013)

precision of the obtained ion concentrations was checked by calculating the ionic balance errors, which were generally below ±5%.

PMF model

The positive matrix factorization (PMF) model is one of the receptor models recommended by the United States Environmental Protection Agency (US EPA) for source apportionment (Paatero & Tapper 1994; Paatero 1997; Liang *et al.* 2017; Guan *et al.* 2018). The PMF 5.0 program requires two input files: one for concentrations of each sample species and the other for the uncertainty values of each sample species. Before applying PMF, the dataset must follow a normal distribution and the outliers (two times or more of the variance) are ignored (Hu & Cheng 2016; Goodarzi *et al.* 2017; Guan *et al.* 2018).

Health risk assessment

Fluoride is ingested mainly through groundwater, food, breathing, and dermal absorption such as during bathing (Aghapour *et al.* 2018; Dehbandi *et al.* 2018; Emenike *et al.* 2018). As groundwater is the main contributor to F^- intake, the health risk assessment conducted in this study only evaluates the risk associated with drinking groundwater.

The RBCA model was employed using Equations (1) and (2) (Brindha *et al.* 2016; Aghapour *et al.* 2018; Emenike *et al.* 2018; Enalou *et al.* 2018; Yousefi *et al.* 2018):

$$ED = C \times IR \quad (1)$$

and

$$ADD = ED/BW \quad (2)$$

where ED is the estimated chronic daily exposure dose of F^- through ingestion of groundwater (mg/d); ADD is the estimated daily intake of F^- through ingestion of groundwater (mg/kg/d), C is the F^- concentration in groundwater (mg/L), IR is the rate of groundwater ingestion (L/d), and BW is the mean body weight (kg).

The health risk of F^- through ingestion of drinking groundwater can be calculated using Equation (3) (EPA 2011; Enalou *et al.* 2018):

$$HQ = ADD/R_{fd} \quad (3)$$

where HQ is the health risk quotient, and R_{fd} is the reference dose of F^- through ingestion of groundwater (mg/kg/d). If $HQ < 1.00$, the health risk of F^- intake through drinking groundwater is negligible; if $HQ > 1.00$, the health risk of F^- intake cannot be ignored. Generally, the higher the HQ value, the higher the health risk (Enalou *et al.* 2018; Yousefi *et al.* 2018).

Considering the significant differences in health risks to people of different ages, the population was divided into the following five groups: infants (0–0.5 years old), children (0.5–10 years old), teens (11–18 years old), male adults (18–70 years old), and female adults (18–70 years old). The IR, BW, and R_{fd} values are listed in Table 2.

Table 2 | Reference dose (R_{fd}), body weight (BW) and ingestion rate (IR water) used in the present studies

Parameters	Distribution type	Units	Value	References
IR	Infants	L/Day	0.25	Dehbandi *et al.* (2018)
	Children		1.50	Dehbandi *et al.* (2018)
	Teens		1.70	Aghapour *et al.* (2018)
	Male		3	Dehbandi *et al.* (2018)
	Female		2.30	Aghapour *et al.* (2018)
BW	Infants	kg	6	Aghapour *et al.* (2018)
	Children		20	Aghapour *et al.* (2018)
	Teens		54	Aghapour *et al.* (2018)
	Male		75	Aghapour *et al.* (2018)
	Female		69	Aghapour *et al.* (2018)
R_{fd}	Reference dose	mg/kg/day	0.06	Aghapour *et al.* (2018), Emenike *et al.* (2018), Enalou *et al.* (2018), Yousefi *et al.* (2018)

Statistical and spatial analyses

A descriptive statistical analysis and FA were conducted using Origin 9.0 and SPSS 19.0 (IBM, USA). The source apportionment of F^- was carried out by PMF 5.0 (US EPA). The spatial variation of fluoride, calcium, and bicarbonate distribution was evaluated by using a spatial analyst module in ArcGIS 9.3 software (ESRI, Redlands, California, USA). An inverse distance weighting (IDW) interpolation method and the best prediction models was used for concentration zoning map of fluoride, calcium, and bicarbonate in the study area.

Descriptive data such as mean, range, and standard deviation were calculated (Table 3). The FA was then applied to obtain relationship information from the obtained data (Table 4). Finally, ArcGIS was used to determine the spatial distribution of geochemical ion contents in the study area (Figure 2).

RESULTS

Geochemical characterization

Geochemical data for the groundwater samples are shown in Table 3. The pH values of the water samples range from 7.20 to 8.28, with a mean value of 7.88, indicating that the water body is a weakly alkaline environment. In addition, the pH values of the water samples are within the acceptable range (6.5–8.5) according to China's national standards for drinking water. Values for TDS range between 319 mg/L and 1,563 mg/L, with a mean value of 975 mg/L. The TDS values in 65.00% of the samples exceed the acceptable limit (1,000 mg/L) according to China's national standard for drinking water while, based on WHO's guidelines for drinking-water quality, the TDS values in 90.00% of the samples exceed the acceptable limit (500 mg/L). The mean cation and anion contents show the following decreasing trends: $Na^+ > Mg^{2+} > Ca^{2+} > K^+$ and $HCO_3^- > SO_4^{2-} > Cl^- > NO_3^- > F^-$. The mean Na^+, Mg^{2+}, Ca^{2+}, and K^+ concentrations are 153.76 mg/L, 50.03 mg/L, 37.98 mg/L, and 0.49 mg/L, respectively. The concentrations of HCO_3^-, SO_4^{2-}, and Cl^- are 518.36 mg/L, 195.42 mg/L, and 71.61 mg/L, respectively.

The F^- concentrations in the groundwater samples range from 0.16 to 2.06 mg/L, with a mean value of 1.10 mg/L. Among these samples, 53.33% have elevated F^- contents that exceed China's national standards for drinking water (1.00 mg/L), and 20.00% of the samples have F^- contents above the WHO's recommended limit (1.50 mg/L) (WHO 1984).

Table 3 | Geochemical data of the samples collected in this study (mg/L, except for pH)

	Mean	Standard deviation	Maximum	Minimum	WHO (2016)	China national drinking-water standard	Percentage (%) of samples exceeding WHO standard	Percentage (%) of samples exceeding China national drinking-water standard
pH	7.88	0.32	8.28	7.20	6.5–8.5	6.5–8.5	0	0
Na^+	153.76	78.60	299.71	20.32	200	200	26.67	26.67
K^+	0.49	0.91	4.11	0.23	/**	/	/	/
Ca^{2+}	37.98	14.15	76.01	19.04	75	/	3.33	/
Mg^{2+}	50.03	18.85	94.49	26.55	30	/	86.67	/
Cl^-	71.61	47.01	188.99	11.71	250	250	0	0
SO_4^{2-}	159.42	133.75	462.39	12.03	200	250	26.67	20.00
HCO_3^-	518.36	144.72	853.02	300.61	200	/	100.00	/
F^-	1.10	0.49	2.06	0.16	1.50	1.00	20.00	53.33
NO_3^-	1.31	2.26	8.51	0*	50	10	0	0
TDS	975	311.78	1,563	319	500	1,000	90.00	65.00

*Zero was set for values less than the limit of detection (LOD).
**'/' represents no standard.

Table 4 | Inter-elemental correlation matrix of dissolved ions ($n = 30$)

	pH	Na^+	K^+	Ca^{2+}	Mg^{2+}	Cl^-	SO_4^{2-}	HCO_3^-	F^-	NO_3^-	TDS
pH	1.00										
Na^+	0.51	1.00									
K^+	−0.63	−0.46	1.00								
Ca^{2+}	−0.02	−0.48	−0.10	1.00							
Mg^{2+}	−0.31	0.01	0.05	0.40	1.00						
Cl^-	0.14	0.55	−0.22	0.60	0.44	1.00					
SO_4^{2-}	0.25	0.67	−0.27	0.66	0.46	0.66	1.00				
HCO_3^-	0.41	0.40	−0.39	−0.44	−0.33	−0.14	−0.16	1.00			
F^-	0.63	0.25	−0.43	−0.78	−0.10	0.03	−0.03	0.63	1.00		
NO_3^-	0.31	−0.16	−0.22	0.04	−0.24	−0.21	−0.12	−0.07	0.35	1.00	
TDS	0.64	0.89	−0.54	0.25	0.11	0.53	0.68	0.54	0.45	−0.09	1.00

Spatial distribution analysis

Spatial variations of the concentrations of F^- and other geochemical ions in groundwater in the Sulin coal district are plotted in Figure 2. The groundwater in the middle and northeastern parts of the study region, including Xutong, Jougou, Wugou, Yuanyi, Tongting, Suntong, Yangliu, Taoyuan, and Zhuxianzhuang, is characterized by elevated F-content (>1.0 mg/L), as shown in Figure 2(b). Only three districts, Wugou, Jiegou, and Taoyuan, have F^- concentrations exceeding the WHO's recommended limit (1.50 mg/L) for drinking water.

The F^- concentrations of groundwater range from 0.16 to 2.06 mg/L in the rainy seasons, which were generally higher than those in the dry seasons in Table 1. This is to be expected because the stronger water–rock interaction will dissolve more F^- into groundwater. Figure 3 indicates that 92.86% of higher fluoride groundwater samples (>1.00 mg/L) are enriched ranging from −135 to −110 m depth. In contrast, the wells with depth lower than 120 m have groundwater with relatively low fluoride. The fact of variation in the concentration of fluoride with depth may indicate that geogenic factors play a significant role (Dehbandi *et al.* 2018; Ali *et al.* 2019).

A GIS tool was utilized to study the spatial variation of F^-, Ca^{2+}, and HCO_3^- concentrations in Figure 2. The GIS technique usually synthesizes available water quality data and predicts unknown data for summarizing overall water quality conditions into an easily understood format (Tiwari *et al.* 2016; Emenike *et al.* 2018). As shown in Figure 2, 48.47% of the study area has F^- concentrations below 1.00 mg/L; 41.65% of the study area has F^- concentrations in the range 1.00–1.50 mg/L; 9.88% of the study area has F^- concentrations above 1.50 mg/L. In other words, 51.53% of the study area shows high F^- groundwater concentrations (exceeding China's national permissible limit of 1.00 mg/L), posing the high health risks of dental and skeletal fluorosis.

Both F^- and HCO_3^- show similar spatial distributions, while F^- and Ca^{2+} have opposite spatial distributions. In addition, F^- concentrations in groundwater are positively correlated with HCO_3^- concentrations, but negatively correlated with Ca^{2+} concentrations (Table 3). This phenomenon suggests that HCO_3^- and Ca^{2+} are the main geochemical factors for F-enrichment.

DISCUSSION

Factor analysis

Factor analysis was employed to determine the relationship between F^- and other constituents to track the geochemical behavior of F^- (Keshavarzi *et al.* 2010; Tiwari *et al.* 2016; Enalou *et al.* 2018). The F^- concentration shows moderate positive relationships (>0.50) with the pH value ($R = 0.63$) and the HCO_3^- concentration ($R = 0.63$), suggesting that

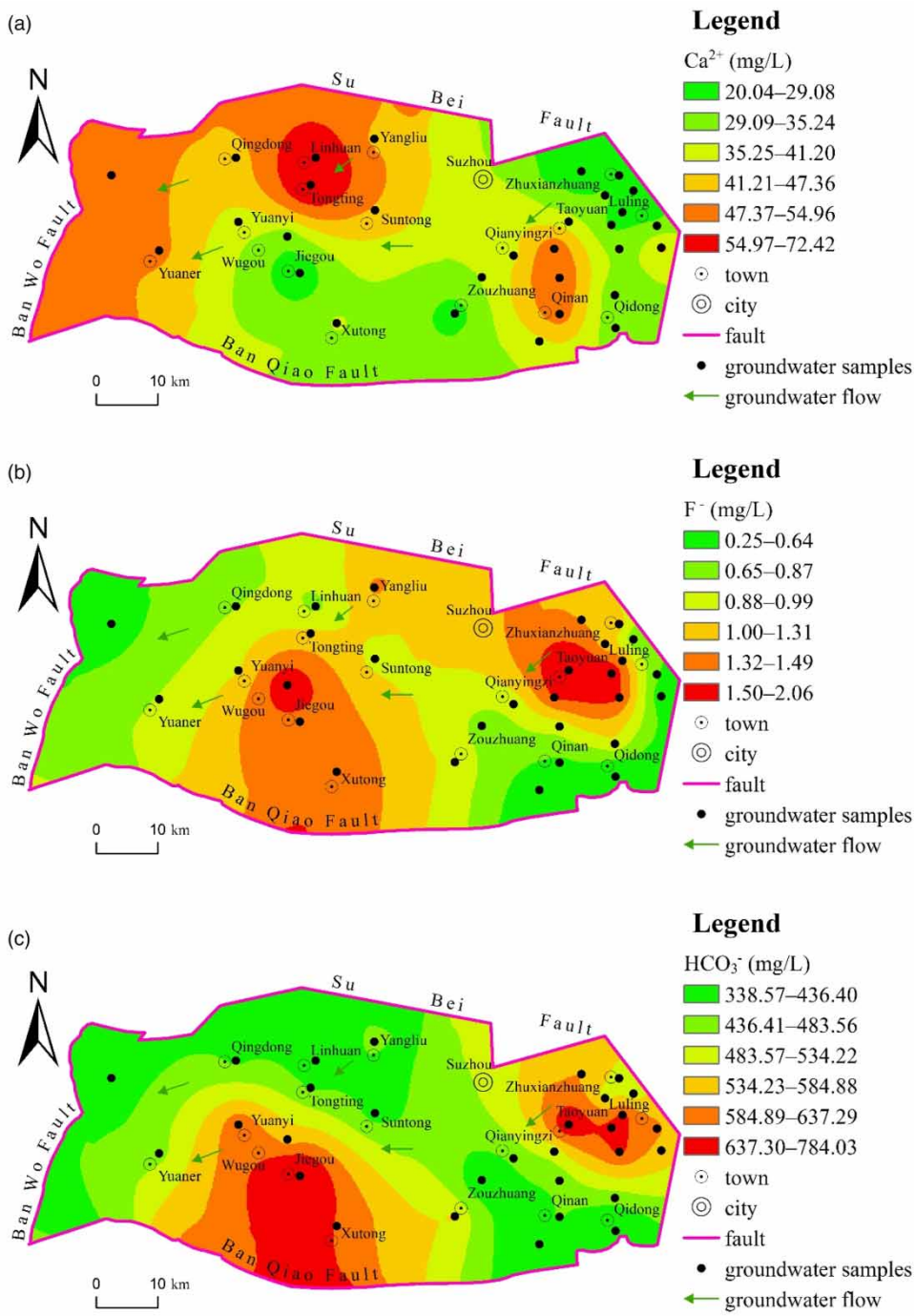

Figure 2 | Spatial distribution of F^- and other ions in the drinking groundwater in the Sulin coal district.

pH and HCO_3^- are important factors for the formation of high F^- groundwater. A positive correlation ($R = 0.41$) was observed between the pH value and the HCO_3^- concentration, as shown in Table 4. This behavior is due to the dissolution of CO_2, resulting in an alkaline environment in drinking-water aquifers with an elevated pH value and an increased HCO_3^- concentration. This indicates that an alkaline environment promotes an increase in F^- in drinking

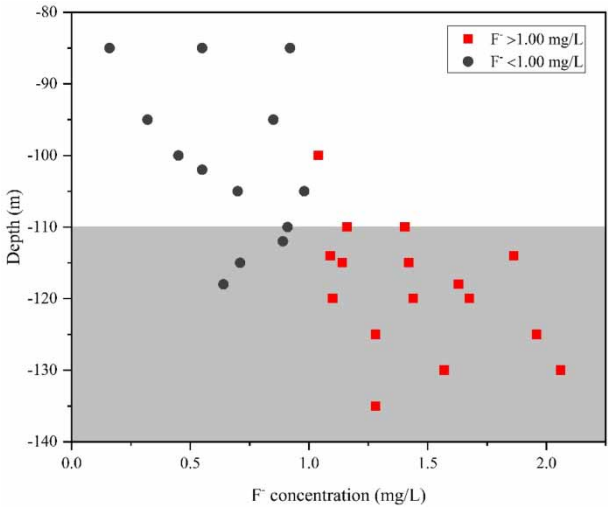

Figure 3 | Variation in F^- concentration in groundwater with depth of wells in the Sulin coal district.

water (He *et al.* 2013b; Goodarzi *et al.* 2017; Raj & Shaji 2017; Ali *et al.* 2019). Furthermore, the F^- concentration has a weak correlation with the TDS value ($R = 0.45$), implying that a high TDS value promotes the weathering of F-bearing minerals and release of F^- into the groundwater (Brindha *et al.* 2016; Dehbandi *et al.* 2018). Generally, evaporation and water–rock interaction can increase the TDS value (Gibbs 1970; Raj & Shaji 2017; Li *et al.* 2018). As the study area is located in an arid or semi-arid zone, hot and dry weather leads to a higher evaporation rate, resulting in a high TDS values in the groundwater.

The concentration of F^- shows a strong negative correlation ($R = -0.78$) with the Ca^{2+} concentration, a negative correlation ($R = -0.10$) with the Mg^{2+} concentration, and a positive correlation ($R = 0.25$) with the Na^+ concentration, suggesting that F^- mainly originates from the weathering of F-bearing minerals, such as fluorite (CaF_2), fluorapatite ($Ca_5(PO_4)_3F$), biotite ($K(Mg,Fe)_3(AlSi_3O_{10})(OH,F)$), phlogopite ($KMg_3(AlSi_3O_{10})$), and hornblende ($CaNa(Mg, Fe, Al)(Si_7Al)O_{22}(OH, F)_2$) (Abu Rukah & Alsokhny 2004; Li *et al.* 2015; Brindha *et al.* 2016; Thapa *et al.* 2018). Additionally, the correlation coefficient between F^- and Ca^{2+} is lower than that between F^- and Mg^{2+}, suggesting that fluorite (CaF_2) and fluorapatite ($Ca_5(PO_4)_3F$) might be the major dissolved F-bearing minerals. A negative correlation ($R = -0.48$) between the concentrations of Ca^{2+} and Na^+ suggests that cation exchange between Ca^{2+} in groundwater and Na^+ in clay plays a significant role during the formation of high F^- groundwater (Li *et al.* 2015; Goodarzi *et al.* 2017; Enalou *et al.* 2018). The positive correlation ($R = 0.35$) between the F^- concentration and the NO_3^- concentration indicates that anthropogenic activities are another important factor in the formation of high F^- groundwater (Sharma & Subramanian 2008; Li *et al.* 2018).

Source apportionment by PMF

The concentrations and uncertainties of F^- and other geochemical ions obtained from 30 groundwater samples were fed into the PMF 5.0 model. Factor number, random start seed number, and run number were optimized to 4, 20, and 10, respectively.

As shown in Figure 4, factor 1 is only predominantly loaded on NO_3^- (86.50%). The primary sources of NO_3^- in groundwater are industrial pollution, agricultural activities, urban solid waste, and coal mining (Heaton 1986; Sharma & Subramanian 2008; Enalou *et al.* 2018). Most of the Sulin coal district consists of farmland and coal mines. No other industry or urban solid waste processing plants were found in the study area. Moreover, based on previous studies, coal mining activities have a minor influence on drinking-water aquifers in this area (Lin *et al.* 2014; Yang *et al.* 2017; Qiu *et al.* 2019). In this regard, factor 1 is related to agricultural activity sources, such as untreated irrigation water, the infiltration of organic matter, synthetic fertilizers, and the runoff from surrounding farmland.

Factor 2 shows strong loadings for SO_4^{2-} (85.60%) and Cl^- (74.40%), and moderate loadings for Ca^{2+} (44.90%), Mg^{2+} (40.00%), and Na^+ (38.50%). The positive loading values for Na^+, Mg^{2+}, and Ca^{2+} suggest that their presence in groundwater is possibly due to weathering and dissolution of minerals (Keshavarzi *et al.* 2010; Kumar *et al.* 2018). The loading value for HCO_3^- (8.50%) is much lower than that for SO_4^{2-} and Cl^-, implying that geochemical processes are dominated by evaporation (Currell *et al.* 2011; Goodarzi *et al.* 2017; Enalou *et al.* 2018). Therefore, factor 2 represents natural geochemical process sources such as evaporation.

Factor 3 is dominated by K^+ (58.20%) and Ca^{2+} (42.80%). As shown in Figure 3, the loading values for all anions in the water samples are negligible and Na^+ has the lowest loading value among the cations, suggesting cation

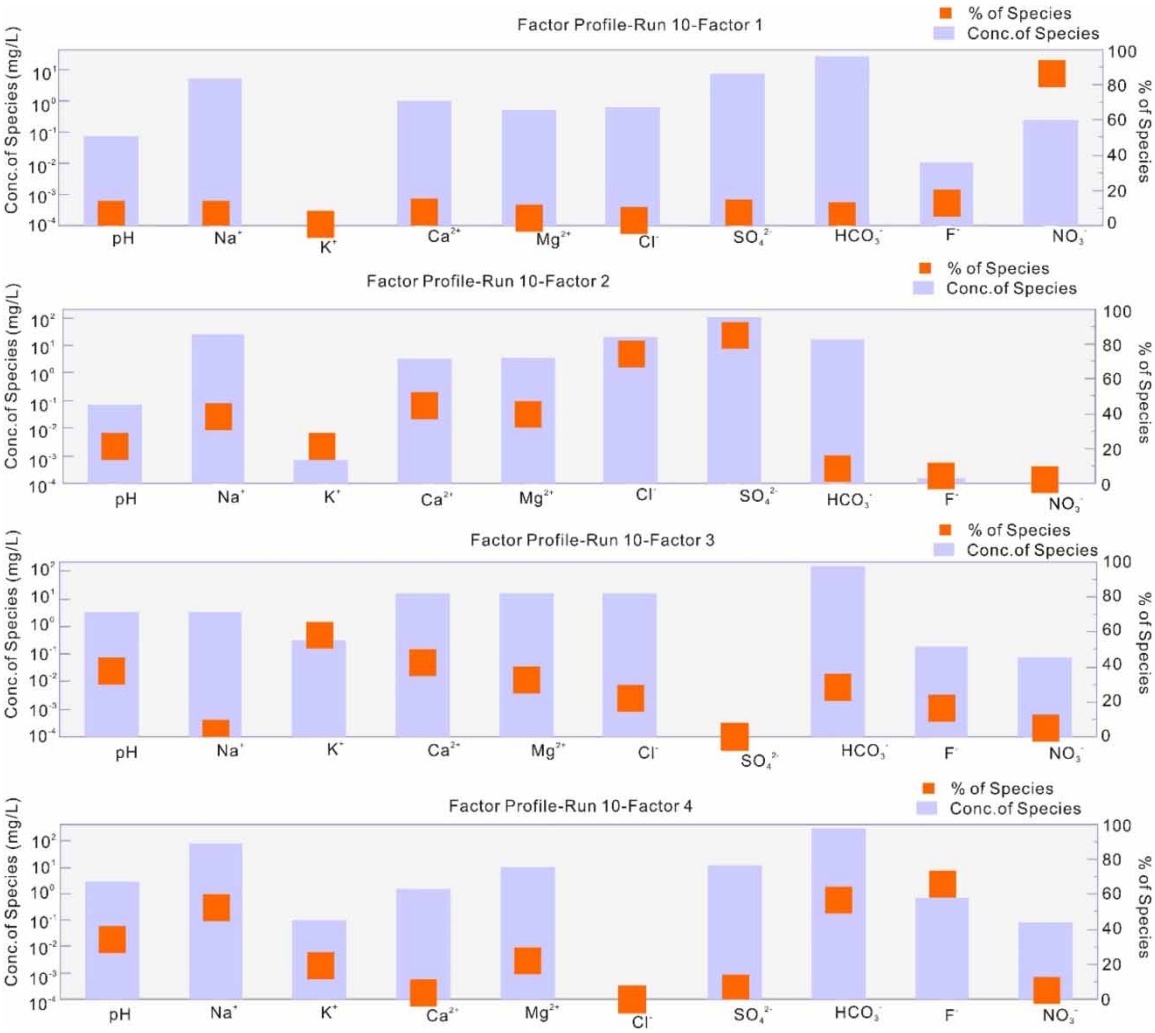

Figure 4 | Factor profiles of F^- sources calculated by PMF model.

exchange between Na^+ in the groundwater and Ca^{2+} or Mg^{2+} in clay or amorphous silicate minerals in groundwater aquifers (He *et al.* 2013b; Li *et al.* 2015; Enalou *et al.* 2018). Hence, factor 3 is associated with a cation exchange source.

Factor 4 shows weights of 66.20%, 57.00%, 52.80%, and 34.20% for F^-, HCO_3^-, Na^+, and pH, respectively. The high loading values for F^-, HCO_3^-, and Na^+, and the low loading value for Ca^{2+} indicate that the F^- concentration in groundwater is controlled by the weathering of F-bearing minerals (Brahman *et al.* 2013; Ali *et al.* 2019). In the study area, rocks, such as granodiorite, porphyrite, amphibolite, and phosphorite, contain a wide variety of F-bearing minerals, including fluorite, hornblende, and phlogopite (Yang *et al.* 2017; Qiu & Gui 2019).

According to the factor fingerprints, the overall percent contribution from each source was computed, as shown in Figure 5. The main source of F^- in the groundwater samples is the weathering of F-bearing minerals, accounting for 66.20%, followed by cation exchange (16.30%), agricultural activities (13.20%), and natural geochemical processes (4.30%). Overall, geological processes, including the weathering of F-bearing minerals, cation exchange, and other geochemical processes are the predominant factors influencing the F^- concentration in groundwater in the Sulin coal district. Surprisingly, agricultural activities contribute approximately 13.20% to the F^- concentration in groundwater in the study area.

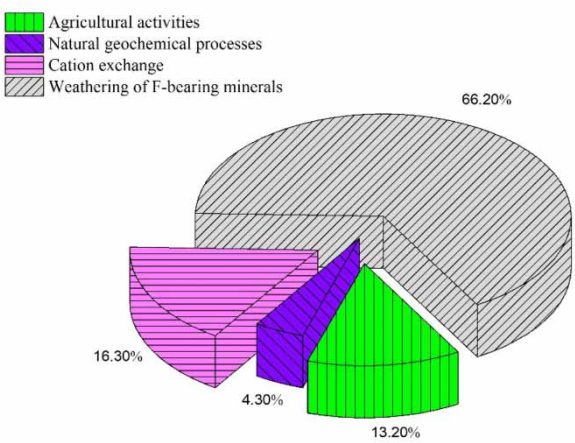

Figure 5 | Factor contributions of F^- sources calculated by PMF model.

Health risk evaluation

In this study, the ED and HQ of F^- caused by ingestion of drinking water are listed in Table 5. According to the Higher French Council for Public Health (CSHPF), the recommended maximum ED of F^- for adults (including males and females), children (including children and teens), and infants are 4, 0.70, and 0.40 mg/d, respectively (Hercberg 2001; Guissouma *et al.* 2017). As shown in Figure 6, the percentage of children whose ED exceeds the maximum ED recommended by CSHPF is the highest, reaching 86.87%, followed by teens (83.33%), male adults (30.00%), infants (13.33%), and female adults (10.00%). This observation suggests that children and teens are more vulnerable in a high F^- environment than other age groups.

Table 5 | ED, ADD, and HQ for different age groups

Types		Mean	Standard deviation	Maximum	Minimum
Infants	ED	0.27	0.12	0.52	0.04
	ADD	0.05	0.02	0.09	0.01
	HQ	0.76	0.34	1.43	0.11
Children	ED	1.64	0.73	3.09	0.24
	ADD	0.08	0.04	0.15	0.01
	HQ	1.37	0.61	2.58	0.20
Teens	ED	1.86	0.83	3.50	0.27
	ADD	0.03	0.02	0.06	0.01
	HQ	0.57	0.26	1.08	0.08
Male	ED	3.28	1.47	6.18	0.48
	ADD	0.04	0.02	0.08	0.01
	HQ	0.73	0.33	1.37	0.11
Female	ED	2.52	1.12	4.74	0.37
	ADD	0.04	0.02	0.07	0.01
	HQ	0.61	0.27	1.14	0.09

The percentages of infants, children, teens, male adults, and female adults, whose F^- intake exceeds the HQ safety limit (1.00) are 20.00%, 70.00%, 6.67%, 20.00%, and 10.00%, respectively, as shown in Figures 7 and 8. The HQ value for children is the highest among all population groups, followed by infants, male adults, female adults, and teens. These results indicate that children are the most vulnerable population group and that they are more likely to suffer from health complications associated with the consumption of high F^- water (Guissouma *et al.* 2017; Emenike *et al.* 2018). This is possibly due to the amount of dietary F^- intake, which is almost twice as high for children than for adults (Battaleb *et al.* 2013; Aghapour *et al.* 2018). Interestingly, as shown in Figure 6, teens have the lowest F^- intake risk, which may be related to the lower intake of local drinking water (Guissouma *et al.* 2017).

As can be seen from Figure 8, infants and male adults with HQs > 1.00 live mostly in Wugou, Taoyuan, and Xutong; teens and female adults with HQs > 1.00 are located in Wugou. Except for Qinan, Linhuan, and Qidong, the HQ of children in the rest of the Sulin coal district is above 1.00 (Figure 7(c)).

The population in Wugou has the highest ED and HQ values, indicating that the risk of developing dental fluorosis is highest. This result agrees with the high F^- groundwater concentration (1.96 mg/L) in this area.

Studies have shown that the optimal F^- concentration in drinking water in an area is related to its climatic condition. The optimum F^- concentration in water can be calculated by Equation (4) (Aghapour *et al.* 2018; Enalou *et al.* 2018):

$$D = 0.34/[-0.038 + (0.0062 \times Tm)] \quad (4)$$

where D is the optimal amount of F^- in groundwater (mg/L) and Tm is the maximum mean atmospheric temperature (°F).

The mean annual temperature of the Sulin coal district is 14–15 °C (approximately 58.2 °F). According to Equation (4), the optimum F^- content in drinking water in this area is 1.05 mg/L. Therefore, managing the F^- concentration in drinking water is essential to reducing the risk of fluorosis for inhabitants in regions with high F^- groundwater.

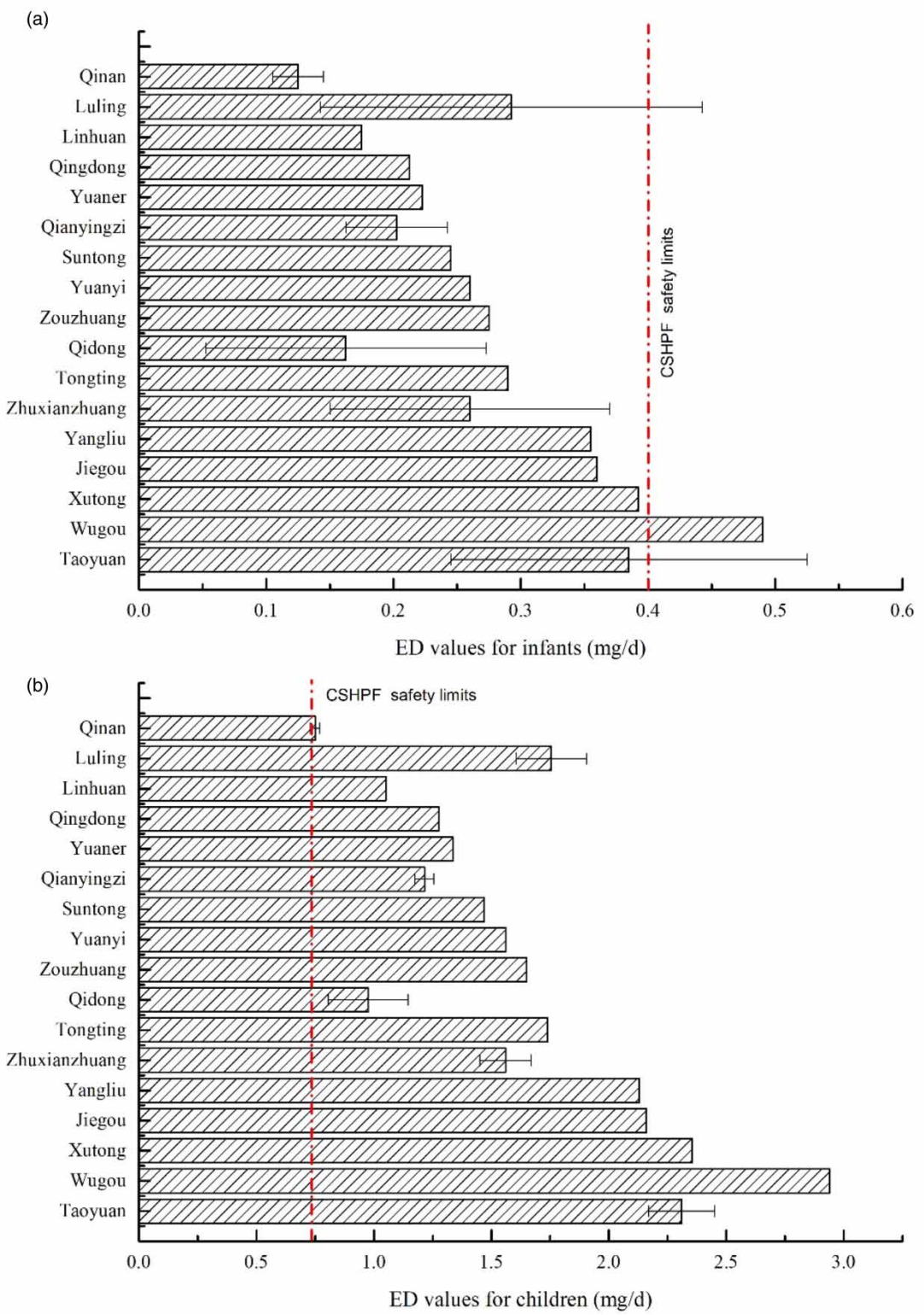

Figure 6 | Diagrams of ED of F^- through ingestion of drinking water for infants (a), children (b), teens (c), male (d), and female adults (e) in the Sulin coal district. *(Continued.)*

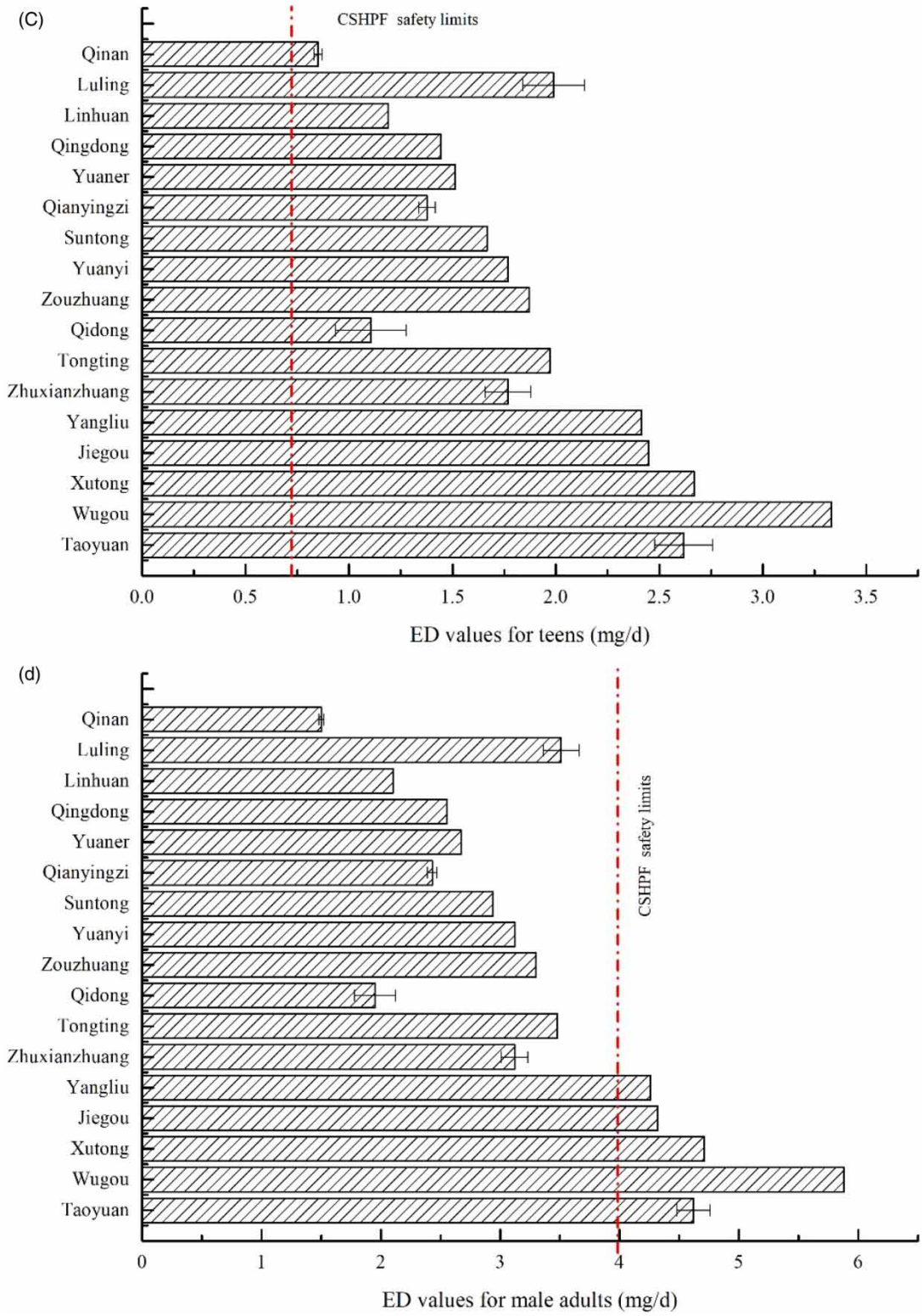

Figure 6 | Continued.

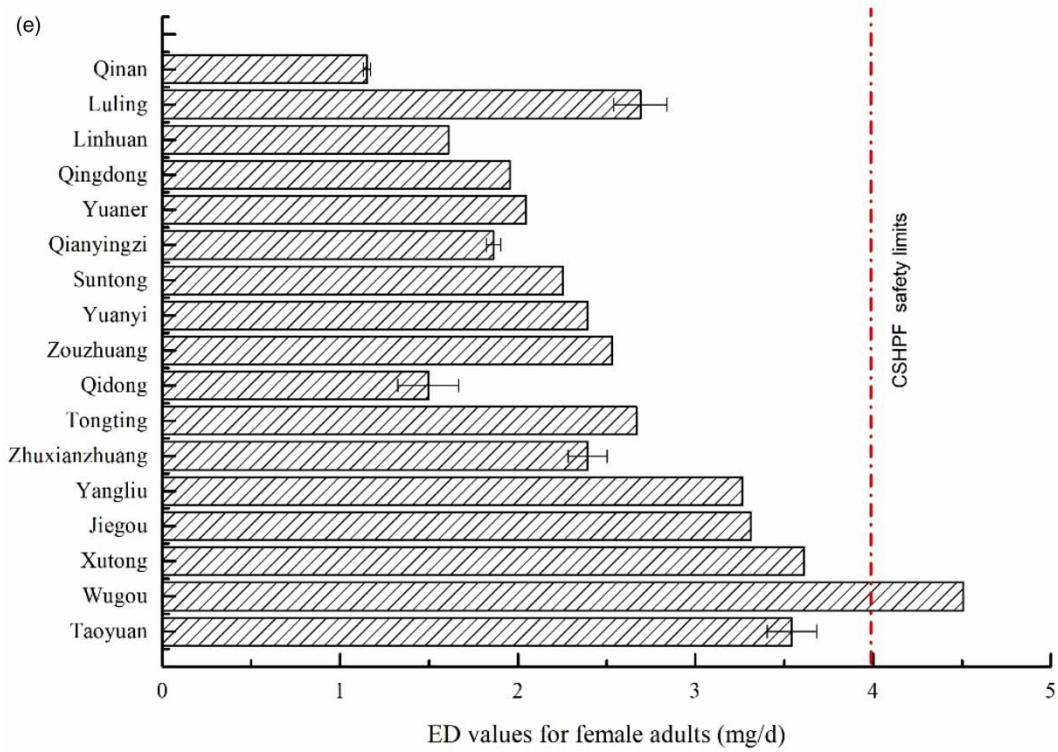

Figure 6 | Continued.

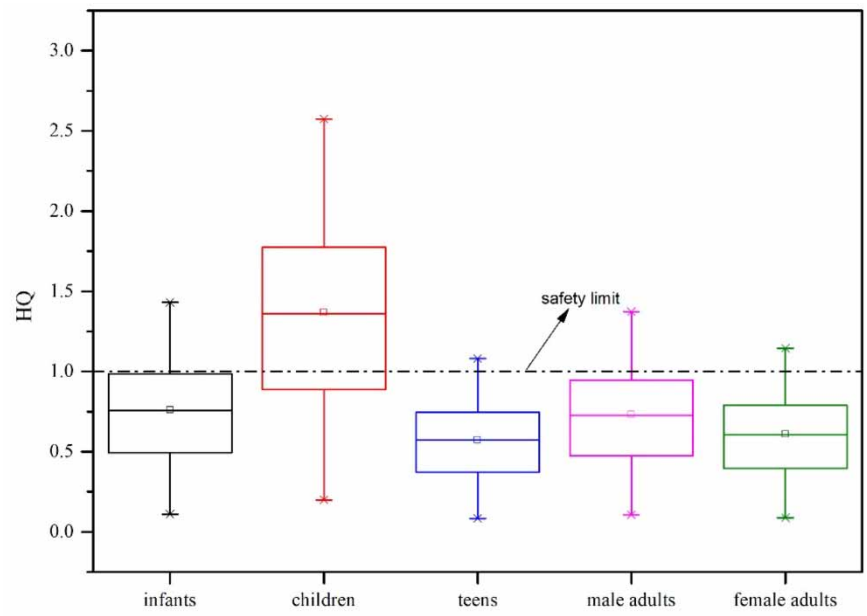

Figure 7 | Boxplots of HQ of F^- through ingestion drinking water for infants, children, teens, male adults, and female adults in the Sulin coal district.

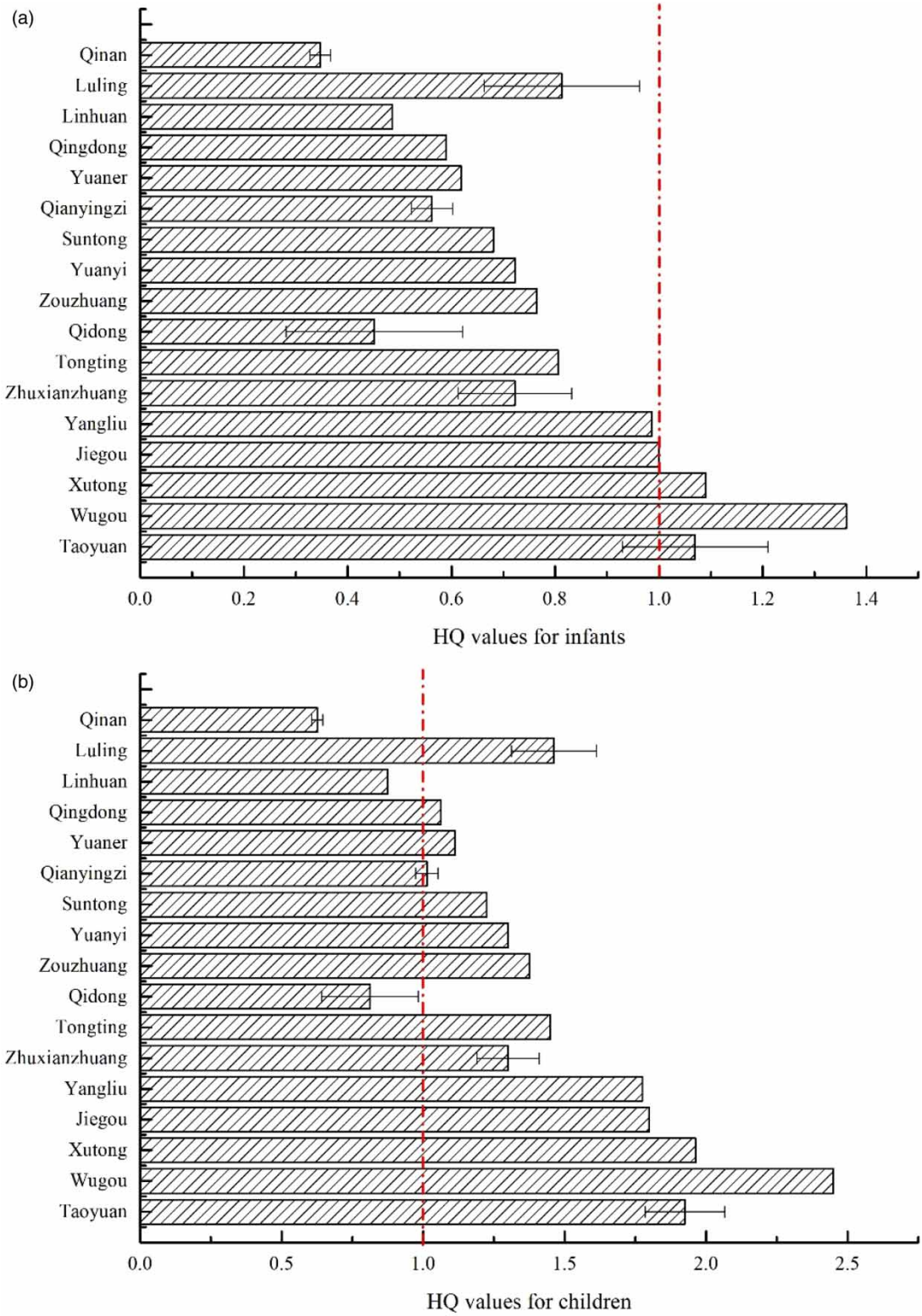

Figure 8 | Diagram of HQ of F^- through ingestion drinking water for infants (a), children (b), teens (c), male (d), and female adults (e) in the Sulin coal district. *(Continued.)*

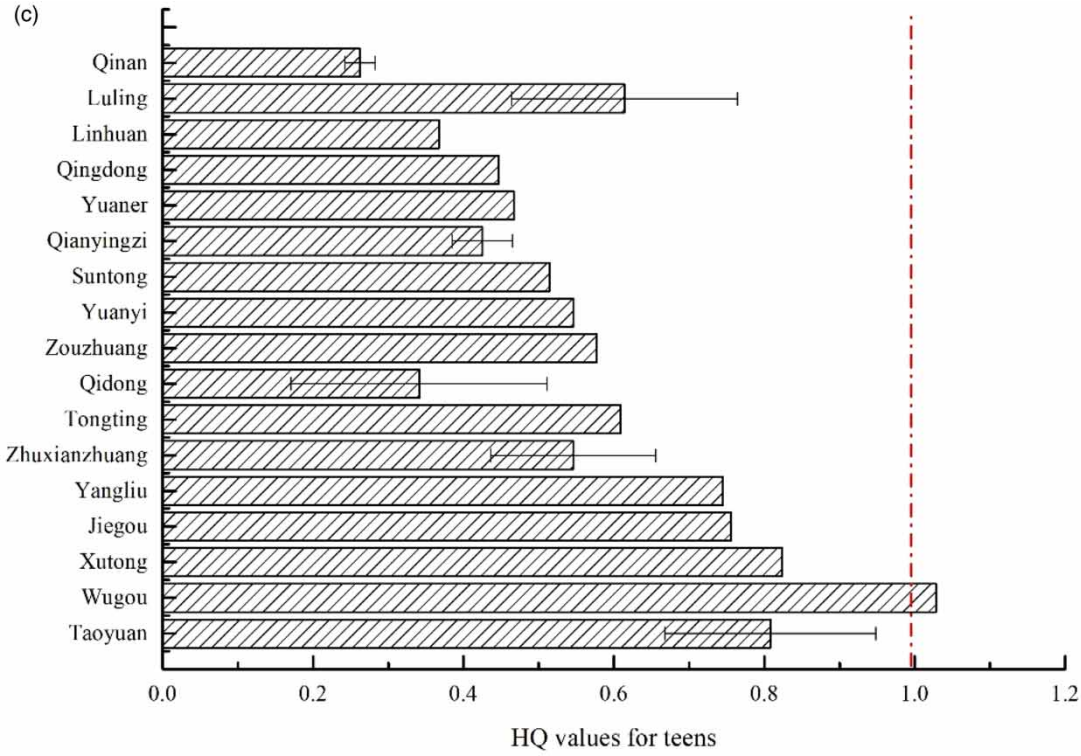

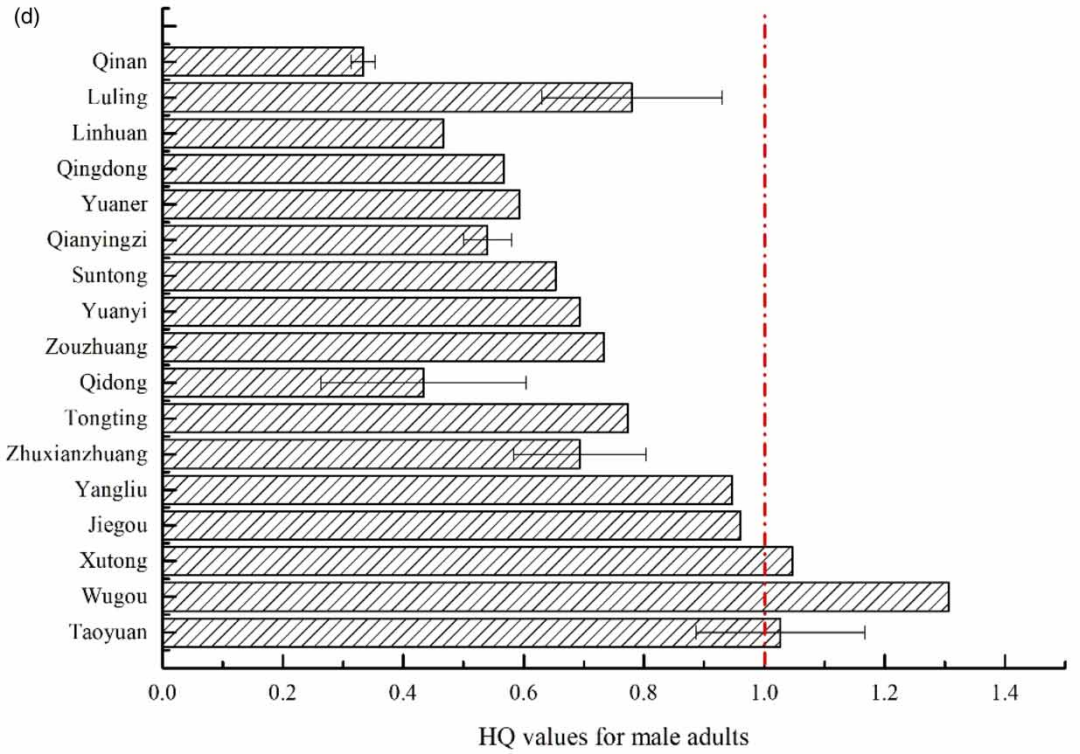

Figure 8 | Continued.

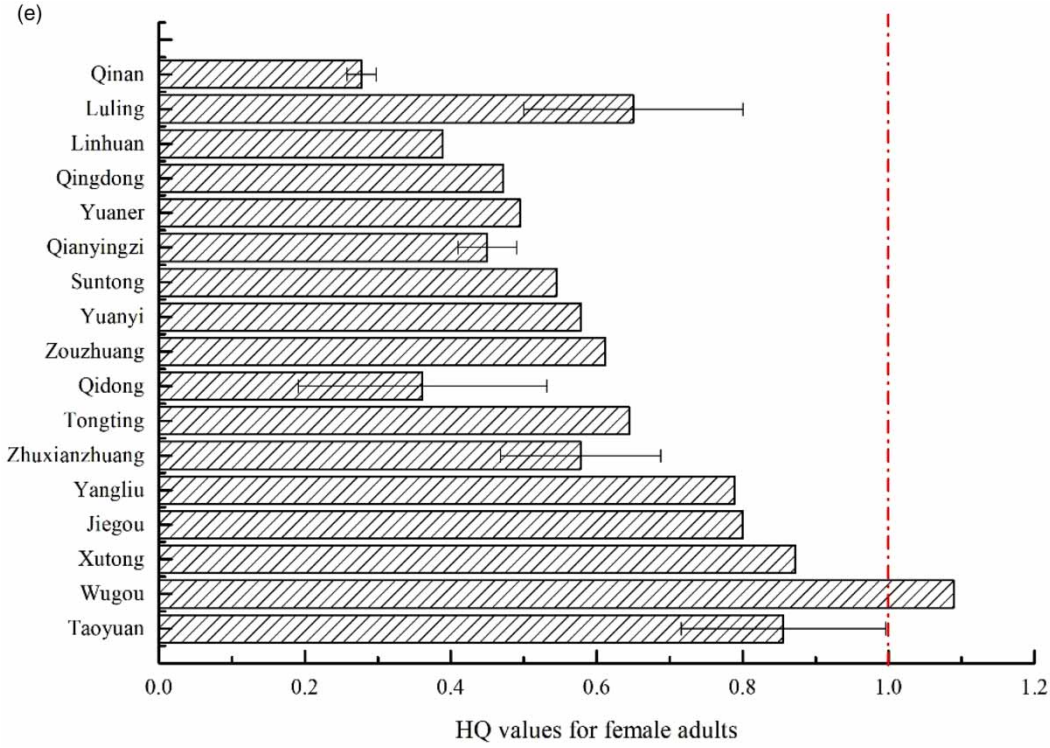

Figure 8 | Continued.

CONCLUSIONS

In this study, content distribution analysis and quantificational source apportionment of F^- in groundwater in the Sulin coal district, northern Anhui Province, China, were carried out. In addition, the health risk assessment of F^- exposure was evaluated for individuals in different groups, such as infants, children, teens, male adults, and female adults. Results can be summarized as follows.

The F^- concentrations in the groundwater samples ranged from 0.16 to 2.06 mg/L, with a mean value of 1.10 mg/L. Among the samples, 53.33% had elevated F^- concentrations, which exceeded China's national standards for drinking water (1.00 mg/L) and 20.00% of the samples showed much higher F^- concentrations beyond the WHO's recommended limit (1.50 mg/L). High F^- groundwater (>1.00 mg/L) was mostly located in the central and the northeastern parts of the study region, including Xutong, Jougou, Wugou, Yuanyi, Tongting, Suntong, Yangliu, Taoyuan, and Zhuxianzhuang. Spatial variations of F^- concentrations revealed that 48.47% of the geographical area had F^- concentrations below 1.00 mg/L, 41.65% of the geographical area had F^- concentration in the range of 1.00–1.50 mg/L, and 9.88% of the geographical area had F^- concentration above 1.50 mg/L.

The F^- concentration in the groundwater samples had a positive relationship with pH, Na^+, and HCO_3^-, and was negatively correlated with Ca^{2+} and Mg^{2+}, indicating weathering of F-bearing minerals as a F^- source. Quantificational source apportionment results explained that the weathering of F-bearing minerals was the main source of F^- in the groundwater samples, accounting for 66.20% of the total dissolved F^-, followed by cation exchange (16.30%), agricultural activities (13.20%), and natural geochemical processes (4.30%).

The percentages of infants, children, teens, male adults, and female adults, whose F^- intake exceeded the HQ safety limit (1.00) were 20.00%, 70.00%, 6.67%, 20.00%, and 10.00%, respectively. With the highest HQ value, children were the most vulnerable age group in high F^- regions. Apart from Qinan, Linhuan, and Qidong, children in the rest of the Sulin coal district were more likely to develop

fluorosis. In addition, infants and male adults in Wugou, Taoyuan, and Xutong, as well as teen and female adults in Wugou, were at high risk of developing fluorosis. Wugou had the highest ED and HQ values due to the high level of F^- in the groundwater of this region. The optimum F^- content in the groundwater of the study region was calculated to be 1.05 mg/L, which provided a reference for local water management authorities to reduce fluorosis caused by excess F^- intake from drinking water.

Despite F^- enriched groundwater in the study area, most residents are not aware of the risks of fluorosis from drinking. Our findings are limited to assisting the informed management of groundwater resources for drinking within the study area. Overall, it is highly suggested for all parts of the geochemical cycle that efforts should be made to find the pathways, mobilization mechanisms, and reduction measures for fluoride that should be taken in the future in efforts to improve public safety.

ACKNOWLEDGEMENTS

The authors gratefully acknowledge the financial support provided by the Open Fund of State Key Laboratory of Groundwater Protection and Utilization by Coal Mining (no. SHJT-17-42.17), the Ecological restoration project in Lengshuijiang Antimony Mine area (no. LCG2020009), and Fundamental Research Funds for the Central Universities of China (no. 3142018011). We would like to thank Editage (www.editage.cn) for English language editing.

DECLARATION OF INTEREST STATEMENT

The authors declare that they have no conflict of interest.

DATA AVAILABILITY STATEMENT

All relevant data are included in the paper or its Supplementary Information.

REFERENCES

Abu Rukah, Y. & Alsokhny, K. 2004 Geochemical assessment of groundwater contamination with special emphasis on fluoride concentration, North Jordan. *Geochemistry* **64** (2), 171–181. https://doi.org/10.1016/j.chemer.2003.11.003.

Aghapour, S., Bina, B., Tarrahi, M. J., Amiri, F. & Ebrahimi, A. 2018 Distribution and health risk assessment of natural fluoride of drinking groundwater resources of Isfahan, Iran, using GIS. *Environ. Monit. Assess.* **190** (3), 137. https://doi.org/10.1007/s10661-018-6467-z.

Ali, W., Aslam, M. W., Junaid, M., Ali, K., Guo, Y., Rasool, A. & Zhang, H. 2019 Elucidating various geochemical mechanisms drive fluoride contamination in unconfined aquifers along the major rivers in Sindh and Punjab, Pakistan. *Environ. Pollut.* **249**, 535–549. https://doi.org/10.1016/j.envpol.2019.03.043.

Battaleb, L., Moore, F., Malde, M. K. & Jacks, G. 2013 Fluoride in groundwater, dates and wheat: estimated exposure dose in the population of Bushehr, Iran. *J. Food Compos. Anal.* **29** (2), 94–99. https://doi.org/10.1016/j.jfca.2012.08.001.

Brahman, K. D., Kazi Afridi, T. G. & Naseem, H. I. 2013 Evaluation of high levels of fluoride, arsenic species and other physicochemical parameters in underground water of two sub districts of Tharparkar, Pakistan: a multivariate study. *Water Res.* **47**, 1005–1020.

Brindha, K., Jagadeshan, G., Kalpana, L. & Elango, L. 2016 Fluoride in weathered rock aquifers of southern India: managed aquifer recharge for mitigation. *Environ. Sci. Pollut. Res. Int.* **23** (9), 8302–8316. https://doi.org/10.1007/s11356-016-6069-7.

Chen, H. Y., Teng, Y. G., Wang, J. S., Song, L. T. & Zuo, R. 2013 Source apportionment of sediment PAHs in the Pearl River Delta region (China) using nonnegative matrix factorization analysis with effective weighted variance solution. *Sci. Total Environ.* **444**, 401–408. https://doi.org/10.1016/j.scitotenv.2012.11.108.

Currell, M., Cartwright, I. & Raveggi, M. 2011 Controls on elevated fluoride and arsenic concentrations in groundwater from the Yuncheng Basin, China. *Appl. Geochem.* **26** (4), 540–552.

Dehbandi, R., Moore, F. & Keshavarzi, B. 2018 Geochemical sources, hydrogeochemical behavior, and health risk assessment of fluoride in an endemic fluorosis area, central Iran. *Chemosphere* **193**, 763–776. https://doi.org/10.1016/j.chemosphere.2017.11.021.

Emenike, C. P., Tenebe, I. T. & Jarvis, P. 2018 Fluoride contamination in groundwater sources in Southwestern Nigeria: assessment using multivariate statistical approach and human health risk. *Ecotoxicol. Environ. Saf.* **156**, 391–402. https://doi.org/10.1016/j.ecoenv.2018.03.022.

Enalou, H. B., Moore, F. & Keshavarzi, B. 2018 Source apportionment and health risk assessment of fluoride in water resources, south of Fars province, Iran: Stable isotopes ($\delta^{18}O$ and δD) and geochemical modeling approaches. *Appl.*

Geochem. **98**, 197–205. https://doi.org/10.1016/j.apgeochem.2018.09.019.

EPA 2011 The United States Environmental Protection Agency. EPA 635/R-03/007. http://www.epa.gov/iris. In support of summary information on the Integrated Risk Information System (IRIS). Exposure Factors Handbook 2011 edition (Final). Washington, DC Chapter 8.

Gao, H. J., Jin, Y. Q. & Wei, J. L. 2013 Health risk assessment of fluoride in drinking water from Anhui Province in China. *Environ. Monit. Assess.* **185** (5), 3687–3695. https://doi.org/10.1007/s10661-012-2820-9.

Gibbs, R. 1970 Mechanisms controlling world's water chemistry. *Science* **170**, 1088–1090.

Goodarzi, F., Mahvi, A. H. & Hosseini, M. 2017 Prevalence of dental caries and fluoride concentration of drinking water: a systematic review. *Dent. Res. J.* **14**, 163–168.

Guan, Q., Wang, F., Xu, C., Pan, N., Lin, J., Zhao, R., Yang, Y. & Luo, H. 2018 Source apportionment of heavy metals in agricultural soil based on PMF: a case study in Hexi Corridor, northwest China. *Chemosphere* **193**, 189–197. https://doi.org/10.1016/j.chemosphere.2017.10.151.

Guissouma, W., Hakami, O., Al-Rajab, A. J. & Tarhouni, J. 2017 Risk assessment of fluoride exposure in drinking water of Tunisia. *Chemosphere* **177**, 102–108. https://doi.org/10.1016/j.chemosphere.2017.03.011.

Guo, H., Zhang, Y., Xing, L. & Jia, Y. 2012 Spatial variation in arsenic and fluoride concentrations of shallow groundwater from the town of Shahai in the Hetao basin, Inner Mongolia. *Appl. Geochem.* **27** (11), 2187–2196. https://doi.org/10.1016/j.apgeochem.2012.01.016.

He, J., An, Y. & Zhang, F. 2013a Geochemical characteristics and fluoride distribution in the groundwater of the Zhangye Basin in Northwestern China. *J. Geochem. Explor.* **135**, 22–30. https://doi.org/10.1016/j.gexplo.2012.12.012.

He, X., Ma, T. & Wang, Y. 2013b Hydrogeochemistry of high fluoride groundwater in shallow aquifers, Hangjinhouqi, Hetao Plain. *J. Geochem. Explor.* **135**, 63–70. https://doi.org/10.1016/j.gexplo.2012.11.010.

Heaton, T. H. 1986 Isotopic studies of nitrogen pollution in the hydrosphere and atmosphere: a review. *Chem. Geol. Isot. Geosci. Sect.* **59**, 87–102.

Hercberg, S. 2001 Les bases de la politique nutritionnelle de santé publique en France: le constat et les recommandations du HCSP. *Oléagineux, Corps Gras, Lipides* **8** (1), 7–12. https://doi.org/10.1051/ocl.2001.0007.

Hu, Y. & Cheng, H. 2016 A method for apportionment of natural and anthropogenic contributions to heavy metal loadings in the surface soils across large-scale regions. *Environ. Pollut.* **214**, 400–409. https://doi.org/10.1016/j.envpol.2016.04.028.

Keshavarzi, B., Moore, F., Esmaeili, A. & Rastmanesh, F. 2010 The source of fluoride toxicity in Muteh area, Isfahan, Iran. *Environ. Earth Sci.* **61** (4), 777–786. https://doi.org/10.1007/s12665-009-0390-0.

Kumar, S., Venkatesh, A. S., Singh, R., Udayabhanu, G. & Saha, D. 2018 Geochemical signatures and isotopic systematics constraining dynamics of fluoride contamination in groundwater across Jamui district, Indo-Gangetic alluvial plains, India. *Chemosphere* **205**, 493–505. https://doi.org/10.1016/j.chemosphere.2018.04.116.

Li, X., Liren, Z. & Xinwei, H. 2007 Distribution and evolutional mechanism of shallow high-fluoride groundwater in Taiyuan Basin. *Acta Geoscientica Sinica* **28** (1), 55–61 (in Chinese).

Li, C., Gao, X. & Wang, Y. 2015 Hydrogeochemistry of high-fluoride groundwater at Yuncheng Basin, northern China. *Sci. Total Environ.* **508**, 155–165. https://doi.org/10.1016/j.scitotenv.2014.11.045.

Li, D., Gao, X., Wang, Y. & Luo, W. 2018 Diverse mechanisms drive fluoride enrichment in groundwater in two neighboring sites in northern China. *Environ. Pollut.* **237**, 430–441. https://doi.org/10.1016/j.envpol.2018.02.072.

Liang, J., Feng, C., Zeng, G., Gao, X., Zhong, M., Li, X., Li, X., He, X. & Fang, Y. 2017 Spatial distribution and source identification of heavy metals in surface soils in a typical coal mine city, Lianyuan, China. *Environ. Pollut.* **225**, 681–690. https://doi.org/10.1016/j.envpol.2017.03.057.

Lin, M., Gui, H. & Peng, W. 2014 Health risk assessment of heavy metals in deep groundwater from different aquifers of a typical coal mining area: a case study of a coal mining area in Northern Anhui Province. *Acta Geosci. Sin.* **35** (5), 589–598. (in Chinese).

Mahvi, A., Goodarzi, F., Hosseini, M., Nodehi, R., Kharazifard, M. & Parvizishad, M. 2016 Fluoride concentration of drinking water and dental fluorosis: a systematic review and meta-analysis in Iran. *Dent. Hypotheses* **7** (3), 81. https://doi.org/10.4103/2155-8213.190482.

Mondal, D., Gupta, S., Reddy, D. V. & Nagabhushanam, P. 2014 Geochemical controls on fluoride concentrations in groundwater from alluvial aquifers of the Birbhum district, West Bengal, India. *J. Geochem. Explor.* **145**, 190–206. https://doi.org/10.1016/j.gexplo.2014.06.005.

Olaka, L. A., Wilke, F. D., Olago, D. O., Odada, E. O., Mulch, A. & Musolff, A. 2016 Groundwater fluoride enrichment in an active rift setting: Central Kenya Rift case study. *Sci. Total Environ.* **545–546**, 641–653. https://doi.org/10.1016/j.scitotenv.2015.11.161.

Paatero, P. 1997 Least squares formulation of robust non-negative factor analysis. *Chemom. Intell. Lab. Syst.* **37** (1), 23–35.

Paatero, P. & Tapper, U. 1994 Positive matrix factorization: a non-negative factor model with optimal utilization of error estimates of data values. *Environmetrics* **5**, 111–126.

Pi, K., Wang, Y., Xie, X., Su, C., Ma, T., Li, J. & Liu, Y. 2015 Hydrogeochemistry of co-occurring geogenic arsenic, fluoride and iodine in groundwater at Datong Basin, northern China. *J. Hazard. Mater.* **300**, 652–661. https://doi.org/10.1016/j.jhazmat.2015.07.080.

Qiu, H. & Gui, H. 2019 Heavy metals contamination in shallow groundwater of a coal-mining district and a probabilistic assessment of its human health risk. *Hum. Ecol. Risk Assess.* **25** (3), 548–563. https://doi.org/10.1080/10807039.2018.1562883.

Qiu, H., Gui, H., Cui, L., Pan, Z. & Lu, B. 2019 Hydrogeochemical characteristics and water quality assessment of shallow groundwater: a case study from Linhuan coal-mining district in northern Anhui Province, China. *Water Supply* **19** (5), 1572–1578. https://doi.org/10.2166/ws.2019.030.

Rafique, T., Naseem, S., Ozsvath, D., Hussain, R., Bhanger, M. I. & Usmani, T. H. 2015 Geochemical controls of high fluoride groundwater in Umarkot Sub-District, Thar Desert, Pakistan. *Sci. Total Environ.* **530–531**, 271–278. https://doi.org/10.1016/j.scitotenv.2015.05.038.

Raj, D. & Shaji, E. 2017 Fluoride contamination in groundwater resources of Alleppey, southern India. *Geosci. Front.* **8** (1), 117–124. https://doi.org/10.1016/j.gsf.2016.01.002.

Rashid, A., Guan, D. X., Farooqi, A., Khan, S., Zahir, S., Jehan, S., Khattak, S. A., Khan, M. S. & Khan, R. 2018 Fluoride prevalence in groundwater around a fluorite mining area in the flood plain of the River Swat, Pakistan. *Sci. Total Environ.* **635**, 203–215. https://doi.org/10.1016/j.scitotenv.2018.04.064.

Rodenburg, L. A., Du, S. & Xiao, B. 2011 Source apportionment of polychlorinated biphenyls in the New York/New Jersey Harbor. *Chemosphere* **83** (6), 792–798.

Sharma, S. K. & Subramanian, V. 2008 Hydrochemistry of the Narmada and Tapti Rivers, India. *Hydrol. Processes* **22** (17), 3444–3455. https://doi.org/10.1002/hyp.6929.

Thapa, R., Gupta, S., Gupta, A., Reddy, D. V. & Kaur, H. 2018 Geochemical and geostatistical appraisal of fluoride contamination: an insight into the quaternary aquifer. *Sci. Total Environ.* **640–641**, 406–418. https://doi.org/10.1016/j.scitotenv.2018.05.360.

Tiwari, A. K., Singh, A. K. & Mahato, M. K. 2016 GIS based evaluation of fluoride contamination and assessment of fluoride exposure dose in groundwater of a district in Uttar Pradesh, India. *Hum. Ecol. Risk Assess.* **23** (1), 56–66. https://doi.org/10.1080/10807039.2016.1220824.

WHO 1984 *Health Criteria and Other Supporting Information*, 2nd edn. World Health Organization, Geneva, Switzerland, pp. 940–949.

Wu, B. R. & Qian, J. Z. 2011 Spatial variation characteristics of fluorine and total dissolved solid in groundwater in Huaibei Plain, Anhui Province. *Sci. Geograph. Sin.* **31** (4), 453–458 (in Chinese).

Wu, B. R., Wang, L. L. & Zhao, W. D. 2010 Distribution rule and sources analysis of high fluorine in shallow groundwater of Huaibei Plain, Anhui Province. *J. Hefei Univ. Technol.* **33** (12), 1862–1865 (in Chinese).

Wu, C., Wu, X., Qian, C. & Zhu, G. 2018 Hydrogeochemistry and groundwater quality assessment of high fluoride levels in the Yanchi endorheic region, northwest China. *Appl. Geochem.* **98**, 404–417. https://doi.org/10.1016/j.apgeochem.2018.10.016.

Yang, N., Liu, J. & Liao, A. 2017 Distribution and formation factors of high fluoride deep groundwater in typical area of north Anhui Province. *Hydrogeol. Eng.-Geol.* **44**, 33–41 (in Chinese).

Yousefi, M., Ghoochani, M. & Hossein Mahvi, A. 2018 Health risk assessment to fluoride in drinking water of rural residents living in the Poldasht city, Northwest of Iran. *Ecotoxicol. Environ. Saf.* **148**, 426–430. https://doi.org/10.1016/j.ecoenv.2017.10.057.

Zhang, S., Liu, G., Sun, R. & Wu, D. 2016 Health risk assessment of heavy metals in groundwater of coal mining area: a case study in Dingji coal mine, Huainan coalfield, China. *Hum. Ecol. Risk Assess.* **22** (7), 1469–1479. https://doi.org/10.1080/10807039.2016.1185689.

First received 30 July 2020; accepted in revised form 5 February 2021. Available online 17 February 2021